Bone 121 (2019) 232–242

Contents lists available at ScienceDirect

Bone

journal homepage: www.elsevier.com/locate/bone

Full Length Article

Intermittent PTH treatment improves bone and muscle in glucocorticoid treated Mdx mice: A model of Duchenne Muscular Dystrophy

Sung-Hee Yoon[a,b], Marc Grynpas[b], Jane Mitchell[a,*]

[a] Department of Pharmacology and Toxicology, University of Toronto, ON, Canada
[b] Lunenfeld-Tanenbaum Research Institute, Mount Sinai Health System, Toronto, ON, Canada

ARTICLE INFO

Keywords:
Mdx mice
Duchenne Muscular Dystrophy
Parathyroid hormone
Glucocorticoids

ABSTRACT

Duchenne Muscular Dystrophy (DMD) is a progressive muscle disorder caused by genetic mutations of the dystrophin encoding gene. In the absence of functional dystrophin, DMD patients suffer from muscle inflammation and wasting, as well as compromised bone health with increased risk of fracture. The use of high dose glucocorticoids (GC) as the standard therapy also contributes to bone fragility. This study examined the effects of intermittent, daily administered parathyroid hormone (iPTH), an approved bone anabolic therapy, on growing bone and dystrophic muscle in the presence and absence of prednisone treatment using the Mdx mouse model of DMD. Five-weeks of prednisone treatment in Mdx mice decreased cortical bone thickness and area ($p < 0.001$), with a large increase in endocortical osteoclasts that were significantly improved by PTH treatment ($p < 0.001$). GC-induced decreases in cortical bone toughness and modulus were improved with iPTH therapy ($p < 0.05$). Mdx mice showed significantly less bone mass in trabecular compartments of lumbar vertebrae and iPTH treatment, with or without glucocorticoids, significantly improved structural and material properties of this bone. Prednisone improved grip strength and endurance of treadmill running, which were maintained and further improved, respectively, in co-treated Mdx mice. Altogether, our study demonstrates that iPTH therapy significantly ameliorated GC-induced bone loss and maintained or further enhanced the positive effects of GCs on dystrophic muscle function. These findings give insight into the potential for use of teriparatide to treat growing bone in children with DMD.

1. Introduction

Duchenne Muscular Dystrophy (DMD) is a X-linked genetic disorder caused by mutations on the dystrophin-encoding gene [1]. As dystrophin is critical in stabilizing the link between the sarcolemma and actin fibers during muscle contractions, DMD patients manifest abnormalities in muscle function as early as 6 months of age. Affecting 1 in 3500 boys, DMD patients have muscle wasting and heightened levels of muscle degeneration and necrosis. Compromised lung function and cardiac failure are the leading causes of death in DMD, usually in the second decade of life if untreated with survival into the third decade under glucocorticoid treatment and supportive therapy [2].

In addition to muscle dysfunction, DMD patients also have poor bone health. Dystrophic muscle itself exerts negative effects on bone, characterized by low bone mineral density (BMD) in femurs and vertebrae and significantly higher fracture rates (up to 44%), especially in the lower extremities [3]. Significantly lower total body and lumbar vertebral BMDs in steroid-naïve DMD patients have been reported [4]. Bone mineral densities of the proximal femur and vertebrae are reduced even further as boys lose ambulation [3]. Thus, it seems that the muscular dystrophy itself intrinsically affects bone negatively in DMD patients.

It has been suggested that increased systemic levels of myokines released from dystrophic muscle could alter bone turnover. Increased levels of interleukin 6 (IL-6) have been shown in serum of patients with DMD as well as Mdx mice and *in vitro* culture of calvaria in media containing 10% sera from Mdx mice increased osteoclasts and bone resorption that could be ameliorated by antibodies that inhibit IL-6 activity [5]. More recently Zhou et al. have assessed the expression of an array of myokines from Mdx mice as well as mice with both dystrophin and utrophin deletion, so called double knockout mice [6]. They have shown large increases in a number of proteins that may influence osteoclasts including IL-6 and leukemia inhibitory factor (LIF) an IL-6 class cytokine that can regulate bone [7] and receptor-activator

* Corresponding author at: Department of Pharmacology and Toxicology, University of Toronto, 1 King's College Circle, Room 4342, Toronto, Ontario M5S 1A8, Canada.
E-mail address: jane.mitchell@utoronto.ca (J. Mitchell).

https://doi.org/10.1016/j.bone.2019.01.028
Received 20 November 2018; Received in revised form 21 January 2019; Accepted 31 January 2019
Available online 01 February 2019

of nuclear factor κ B ligand (RANKL) that is a well known regulator of osteoclastogenesis [8].

To decrease the rate of muscle function loss, most patients commence long-term glucocorticoid therapy once their muscle development has plateaued at around 5 years of age [9]. The prolonged use of glucocorticoids further exacerbates bone loss in DMD patients, with a prominent reduction in lumbar vertebrae BMD (z score of −4 or lower) [4] and low trauma vertebral fracture rates as high as 75% after 100 months of corticosteroid treatment [10]. Studies have reported that glucocorticoid-treated DMD patients had increased vertebral fractures, while long-bone fracture rates were comparable between glucocorticoid-naïve and treated groups [11,12].

Altogether, poor bone health is well recognized in DMD, especially in glucocorticoid-treated patients, the use of additional interventions to help ameliorate the effects of the underlying disease and glucocorticoid therapy in these patients has not been well explored. In our previous studies, we have assessed the efficacy of anti-resorptive bisphosphonates in the Mdx mouse model of DMD. We showed that early administration of bisphosphonates with glucocorticoids could improve bone mineral density and microarchitecture, however, improvement of the biomechanical properties of the bone required pre-treatment with bisphosphonates [13,14]. Suppression of bone formation by glucocorticoids was not improved by bisphosphonates and could limit the longer term efficacy of this approach to osteoporosis treatment [13,14].

An alternative to anti-resorptive therapy is the use of anabolic, intermittent parathyroid hormone (iPTH) treatment that has been used successfully to treat glucocorticoid-induced osteoporosis in adults [15,16]. Teriparatide (PTH 1-34) or abalopeptide (PTH related protein PTHrP) are approved bone anabolic treatments for adult bone health. Both peptides stimulate the PTH1R and when applied intermittently increase bone turnover in favor of bone formation [15]. Glucocorticoids in excess are known to decrease osteoblastogenesis, and cause apoptosis of osteoblasts and osteocytes resulting in severe bone loss and poor bone quality [17]. Teriparatide is effective in treating glucocorticoid-induced osteoporosis in older women, with fewer vertebral fractures and greater improvements in lumbar spine and hip bone mineral densities [16]. Thus, anabolic PTH therapy might be useful in reducing bone loss in glucocorticoid-treated children with DMD but has not been assessed. We have tested this here using iPTH treatment alone or in combination with glucocorticoids in Mdx mice during rapid growth. Mdx mice have an inactivating mutation in the dystrophin gene and show significant decreases in muscle function, although not as profound as that seen in DMD boys [18]. These mice also have cortical bone that is significantly thinned by glucocorticoid therapy, similar to DMD patients, making them a good model for assessment of therapies for treatment of glucocorticoid-induced bone disease [13,14,19]. We show here that co-treatment with iPTH increases the number of osteoblasts and improves bone formation and biomechanical properties in GC-treated Mdx mice during the age of rapid bone growth. At the same time, iPTH co-treatment also enhanced the positive effects of glucocorticoids on muscle function and the types of muscle fibers in Mdx mice.

2. Materials and methods

2.1. Animals and experimental design

Four-week old C57BL/10ScSn-*Dmd*^{mdx}/*J* (Mdx) and C57BL/10SnJ wild-type (WT), male mice were obtained from the Jackson Laboratory (Bar Harbor, ME, USA). After one week of acclimation, mice were randomly assigned into different treatment groups with 10 mice in each group; 1) WT on placebo (PL) pellets with saline injections, 2) Mdx on PL with daily saline injections, 3) Mdx on glucocorticoid (GC) pellets and saline injections, 4) Mdx on PL with daily PTH injections, 5) Mdx on GC and daily PTH injections. At 5 weeks of age, each mouse received a 5 mg, 60 day slow-release pellet of placebo or the glucocorticoid prednisone (Innovative Research, Sarasota, FL, USA) resulting in a prednisone dose of approximately 4.1 mg/kg body weight/day. Glucocorticoid or placebo pellets were inserted into a pocket created under the skin *via* a small incision on the back under sterile conditions with isoflurane anesthesia. Lyophilized rat PTH (1-34) (Bachem Americas, CA) was reconstituted in 10 mM acetic acid in PBS, and diluted to inject approximately 0.1 ml per mouse, at a dose of 150 μg/kg body weight/day. PTH was administered subcutaneously, every day (7 days a week), starting from 3 days post-pellet implantation surgery till the time of the sacrifice at 10 weeks of age. Animals were housed under standard conditions with Teklad Global 14% protein rodent maintenance diet and water *ad libitum*. At the end of the treatments when mice were 10 weeks of age they were euthanized under isoflurane anesthesia with blood collected by cardiac puncture. Serum samples were stored at –80 C until assay for total creatine kinase (CK) activity by assessing the production of NADPH (Beckman Coulter, Mississauga, Canada). All animal care procedures were reviewed and approved by University of Toronto Animal Care Committee.

2.2. Cortical and trabecular bone microarchitecture analyses

The left femur and L6 vertebrae from each mouse were harvested and stored in saline-soaked gauze at −20 °C until testing. Femur lengths were measured using digital calipers (VWR, Mississauga, ON, Canada). For cortical and trabecular bone microarchitecture analyses and volumetric bone mineral density measurements, micro-computed tomography was performed using a SkyScan 1174 (SkyScan, Brucker, Canada). Transverse images were acquired at 50 kV and 800 μA. The mid-diaphysis of femurs were scanned at an isotropic voxel size of 11.6 μm resolution for cortical bone assessment, and distal femurs were scanned at 6.2 μm resolution for trabecular bone assessment. The rotation step sizes used for mid-diaphysis, distal femur and vertebral bones were 0.64, 0.44, and 0.40 degrees, respectively. Two hydroxyapatite phantoms (0.25 g/cm^3 and 0.75 g/cm^3) were scanned daily for calibration after flat-field correction. Scanned images were reconstructed into three-dimensional images and analyzed using the Skyscan CT-Analyzer software (version 1.16). Volumes of interest (VOI) were established as follows: an 86 sections (0.5 mm) VOI at the cortical mid-shaft of the femur for cortical bone, and a 130-section (0.8 mm) VOI measured 270 sections (1.7 mm) from formation of the first cartilage bridge for the trabecular compartment in the femur metaphysis using CTanalyzer software. To delineate bone from soft tissue, global thresholds of 1.1 g hydroxyapatite (HA)/cm^3 (gray value 100) and 0.9 g HA/cm^3 (gray value 65) were used for cortical and trabecular bone analyses, respectively. At the femur mid-diaphysis, volumetric BMD (g/cm^3), cortical bone area (B.Ar, mm^2), cortical thickness (mm), anteroposterior and medio-lateral diameters (mm) were measured. In the distal femurs, trabecular morphometry measurements included the bone volume fraction (BV/TV, %), trabecular thickness (Tb.Th, μm), trabecular number (Tb.N, mm^{-1}), trabecular separation (Tb.Sp, mm), structure model index (SMI), and trabecular bone pattern factor (Tb.Pf). Trabecular pattern factor is a numerical representation of trabecular connectivity. It is based on the concavity and convexity of trabeculae and could predict biomechanical properties. The more trabeculae are connected the more concavity is evident, which results in smaller or negative values, whereas more convexity will give higher pattern factor numbers.

2.3. Biomechanical testing

To determine the biomechanical properties of the cortical bone, three-point bending tests were performed on the excised left femurs. Lumbar vertebral bodies (L6) were used for vertebral compression to test the biomechanical properties of the primarily trabecular bone at this site. Before testing, vertebral processes were removed and the distal end of each vertebral body was fixed to the stage with cyanoacrylate

adhesive. An Instron 4465 testing machine (Instron Corp., Canton, MA, USA) equipped with a 100 N load cell was used for both 3-point bending and vertebral compression tests. With a pre-load of 0.5 N or less, the force applicator was lowered at a constant rate of 1.0 mm/min or 0.5 mm/min for 3-pt bending and vertebral compression tests, respectively. Load–deformation curves were generated on LabView 5.0 data acquisition software (National Instruments Corp., Austin, TX, USA) and ultimate load (N), failure displacement (mm), energy to fail (mJ), and stiffness (N/mm) were measured. These parameters were normalized using relevant femoral and vertebral geometries measured by microCT, giving values of ultimate stress (MPa), failure strain (%), toughness (mJ/mm^3), and Young's modulus (MPa) [20].

2.4. Bone histomorphometry

Following dissection, right femurs were fixed in 70% ethanol for one week at 4 °C, dehydrated in graded acetone, and embedded in spurr resin. Five μm-thick coronal sections were cut using a Leica RM2265 rotary microtome (Leica, Wetzlar, Germany) and stained with Goldner's trichrome. Seven μm-thick coronal sections were left unstained for imaging of calcein fluorescence. To assess dynamic bone histomorphometry, mice were injected subcutaneously with calcein green (0.6% calcein green in water; 30 mg/kg; Sigma-Aldrich, Oakville, ON, Canada) 12 and 2 days, and xylenol orange (0.9% xylenol orange in water; 90 mg/kg; Sigma-Aldrich) 7 days prior to sacrifice [21]. As the trends between the first two and last two injections were comparable, analyses of the last two injections are reported for dynamic histomorphometry.

Left tibiae were fixed in 10% neutral buffered formalin for one week at 4 °C, and decalcified in EDTA (0.5 M, pH 7.4) at 4 °C, until complete decalcification was confirmed by Faxitron imaging (Faxitron Bioptics, Tucson, AZ, USA). Decalcified bones were processed through a graded series of formalin-ethanol solutions and embedded in paraffin. Five μm thick coronal sections and cross sections, for trabecular bone and endocortical bone analyses, respectively, were cut with a Leica Reichert Jung 2030 microtome and tartrate-resistant acid phosphatase (TRAP) stained for osteoclasts using an acid phosphatase leukocyte kit (Sigma-Aldrich) according to the manufacturer's instructions. All slides were scanned at 200× magnification for analyses. Static and dynamic histomorphometric parameters of bone formation and resorption were performed on the trabecular area of the distal femurs using BioQuant Osteo v11.2.6. All histomorphometric measurements were expressed following the guidelines of the American Society of Bone and Mineral Research [22].

2.5. In vitro osteoclastogenesis

Bone marrow stromal cells (BMSCs) were derived from right tibias by flushing the bone marrow under aseptic conditions using αMEM supplemented with an antibiotic-antimycotic (AA) mixture (Life Technologies, Burlington, ON, Canada). Cells were cultured without glucocorticoids or PTH in the same medium with 10% fetal bovine serum (FBS) for 96 h at 37 °C in a humidified 5% CO_2 atmosphere. Non-adherent cells were harvested and plated on 48-well cell culture plates at a density of 0.75×10^6 cells/well, and cultured in αMEM supplemented with 10% FBS, AA, 30 ng/ml M-CSF and 50 ng/ml RANKL (PeproTech, Rocky Hill, NJ, USA) for osteoclast differentiation. The medium was changed every 2 days and on day 7, cells were rinsed and fixed with 10% buffered formalin. Cells were stained for TRAP and counterstained with hematoxylin (Sigma-Aldrich). Cell images were taken at 10× magnification, and osteoclasts were identified as TRAP-positive cells with 3 or more nuclei. Osteoclast surface areas were traced and measured in 5 wells per treatment group, using Nikon Imaging Software NIS-Elements AR v3.22 (Nikon Canada).

2.6. Grip strength test

Weekly grip strength tests were performed using a digital force meter (Columbus Instruments, Chatillon, FL, USA) as a measure of muscle strength. Briefly, each mouse was held by its tail with its front paws placed on the metal grid attached to a force meter. The animal was gently pulled backwards to stimulate the mouse to pull the grid while the peak force during the pull was recorded. Averages of three measurements per mouse each week were used for analysis.

2.7. Treadmill running test

Mice were tested for their fatigue resistance by measuring their running time on a treadmill 3 days before sacrifice, using an ExerGait treadmill (Columbus Instruments, TreadScan™ 1.0 software, CleverSys Inc.). All mice were acclimatized twice to the treadmill, 2 and 4 days before the testing, for 10 min, gradually speeding up to the testing speed of 17 m/min. For the testing, the speed was increased from 6 m/min to 17 m/min over 2 min as a warm-up. Total running time on the treadmill at 17 m/min was measured until fatigue. Fatigue was defined as 1) if the mouse rested > 3 times within 2 min, or 2) if the mouse rested for > 10 s, and would not go back on the treadmill voluntarily. During the warm-up period, the mouse was gently encouraged to run, but not during the actual testing.

2.8. Muscle histology

Diaphragms were harvested and fixed in 10% buffered formalin for 24 h. After a series dehydrations in ethanol, samples were embedded in wax, and five-μm thick sections were stained with hematoxylin and eosin (H&E). The muscle fibers with central nuclei were counted and the percentage of affected muscle fibers was calculated. Fiber size variance coefficient was determined as previously defined [23].

Tibialis anterior muscles were dissected and frozen using isopentane chilled in liquid nitrogen. Sections were selected from the belly of the muscle and stained for ATPase activity to determine muscle fiber types, as instructed previously [24,25], with a modification of using sodium acetate buffer instead of barbital buffer. Five fields of view per sample were selected for analysis on Nikon Imaging Software NIS-Elements AR v3.22 (Nikon Canada).

2.9. RNA extraction and real-time PCR

Quadriceps were dissected and snap-frozen in liquid nitrogen. Tissues in Trizol Reagent (Invitrogen, Mississauga, ON, Canada) were homogenized with a polytron and total RNA was isolated according to the Trizol manufacturer's instructions. 1 μg of RNA was treated with DNAse I (Invitrogen) for 30 min at 37 °C before carrying out reverse transcription with M-MLV reverse transcriptase (Invitrogen) to a final cDNA product volume of 31 μl. Real-time PCR amplification reactions were performed using a Bio-rad CFX96 PCR system in 18 μl triplicate wells containing 1 μl of cDNA product, 0.3 μM of primers, and 10 μl of SYBR-green PCR master mix (Life Technologies). Primers used are shown in Table 1. Gene expressions were analyzed using delta-delta CT method, using a WT sample as the calibrator, and Hprt as the housekeeping gene.

2.10. Statistical analysis

Data are presented as the mean ± standard deviation (SD). Statistical analyses were performed using one-way ANOVA, followed by post hoc Bonferroni test between WT and Mdx mice (WT PL Sal *vs.* Mdx PL Sal), and between different treatment groups of the Mdx mice (Mdx PL Sal *vs.* Mdx GC Sal *vs.* Mdx PL PTH *vs.* Mdx GC PTH). For body weights and grip strengths, two-way ANOVA was used to factor in age as the additional parameter. For biomechanical data in Tables 5 and 6,

Table 1
List of primers used for RT-qPCR.

Gene	Direction	Sequence (5′ to 3′)
Igf2	Forward	AGT TTG TCT GTT CGG ACC GC
	Reverse	AAG CAG CAC TCT TCC ACG AT
Col1a1	Forward	GCC TTG GAG GAA ACT TTG CTT
	Reverse	GCA CGG AAA CTC CAG CTG AT
Postn	Forward	AAG GTG CTA TCT GCG GGA AG
	Reverse	GTC AAT AGG CAT CAC TGC GG
Lgals3	Forward	AAT CAG GAA AAT GGC AGA CAG C
	Reverse	TGA GGG TTT GGG TTT CCA GAG
Spp1	Forward	CTG GCA GCT CAG AGG AGA AG
	Reverse	TTC TGA GAT GGG TCA GGC AC
Fgf21	Forward	GTG TCA AAG CCT CTA GGT TTC TT
	Reverse	GGT ACA CAT TGT AAC CGT CCT C
IL-6	Forward	TAG TCC TTC CTA CCC CAA TTT CC
	Reverse	TTG GTC CTT AGC CAC TCC TTC
IL-1β	Forward	GCA ACT GTT CCT GAA CTC AAC T
	Reverse	ATC TTT TGG GGT CCG TCA ACT
TNFα	Forward	CCC TCA CAC TCA GAT CAT CTT CT
	Reverse	GCT ACG ACG TGG GCT ACA G
Rankl	Forward	GGC CAC AGC GCT TCT CA
	Reverse	CCT CGC TGG GCC ACA TC
Sparc	Forward	GTG AGC TGG ACG AGA GCA AC
	Reverse	AGA AGT GGC AGG AAG AGT CG
Hprt	Forward	GTT TAA GCA GTA CAG CCC CA
	Reverse	TTC AAC ACT TCG AGA GGT CC

Igf2; insulin-like growth factor 2, Col1a1; collagen 1a1, Postn; periostin, Lgals3; galectin-3, Spp1; osteopontin, Fgf-21; fibroblast growth factor-21, IL-6; interleukin-6, IL-1β; interleukin-1 beta, TNFα; tumor necrosis factor alpha, Rankl; receptor activator of nuclear factor kappa-B ligand, Sparc; osteonectin, Hprt; hypoxanthine-guanine phosphoribosyltransferase.

due to large standard deviations, values were logged before one-way ANOVA. The sample size for each treatment group was at least 8, unless otherwise indicated.

3. Results

3.1. Body weights and bone growth

As expected animal body weights increased over time for all groups of mice except the two groups treated with glucocorticoids (Fig. 1A). Glucocorticoid treated animals had 17% decrease in their body weight in the first week of treatment and 22% decrease by the time of sacrifice (Fig. 1A). Although the initial body weight of PTH treated Mdx mice was 8.5% smaller, they were significantly (9%) heavier than the control Mdx group by the end of the treatment period. This may reflect the PTH induced increase in bone mass (Fig. 2, Tables 2–4). The effect of PTH on body weight was minimal in co-treated Mdx group (Fig. 1A).

Femur lengths of Mdx mice were significantly shorter than wild-type mice (Fig. 1B). Longitudinal bone growth was further suppressed in glucocorticoid treated mice but was not affected by PTH treatment.

3.2. Cortical and trabecular microarchitectures

With a significant decrease in anterior-posterior diameter, Mdx mice had significantly reduced bone perimeter compared to WT mice (Fig. 2, Table 2). Glucocorticoid treatment resulted in significant thinning of the cortical bone, whereas PTH treatment increased cortical thickness and bone area, as well as bone diameter. In the presence of glucocorticoids, PTH treatment still improved cortical thickness and bone area (Fig. 2).

In the trabecular compartment of the distal femur, the dystrophic muscle effect on bone was evident. Volumetric BMD, as well as bone mass were negatively affected by dystrophic muscle in Mdx mice (Fig. 2, Table 3). As previously reported [9], the response of this Mdx mouse strain to glucocorticoids is an increase in volumetric BMD and bone mass. The PTH treatment, as expected, resulted in significant increases in volumetric BMD, bone mass, as well as trabecular thickness. In the presence of glucocorticoids, on the other hand, the effect of PTH was blunted in terms of volumetric BMD and trabecular number. However, trabecular thickness and separation were improved with co-treatment to a greater extent than PTH treatment alone, and the percent bone volume was also significantly improved compared to glucocorticoid-treated Mdx mice.

Trabecular bone in lumbar vertebrae also showed an osteopenic phenotype in Mdx mice (Fig. 2, Table 4). The lumbar vertebrae showed minimal effect of glucocorticoids or PTH on trabecular bone, but the combination of both treatments resulted in significant improvement of all parameters. Altogether, PTH treatment significantly improved cortical and trabecular bone, which were compromised by the presence of dystrophic muscle or glucocorticoid treatment.

3.3. Bone biomechanical properties

Although the presence of dystrophic muscle had minimal effect on cortical bone microarchitecture, Mdx femurs were weaker with significantly reduced fail displacement and strain, as well as energy to fail and toughness (Table 5). With glucocorticoid treatment, energy to fail, toughness, stiffness and modulus were negatively affected, and these were all significantly improved by PTH treatment, with or without glucocorticoids (Table 5).

A biomechanical effect of the osteopenic phenotype in the lumbar vertebrae of Mdx mice was observed with decreased ultimate load,

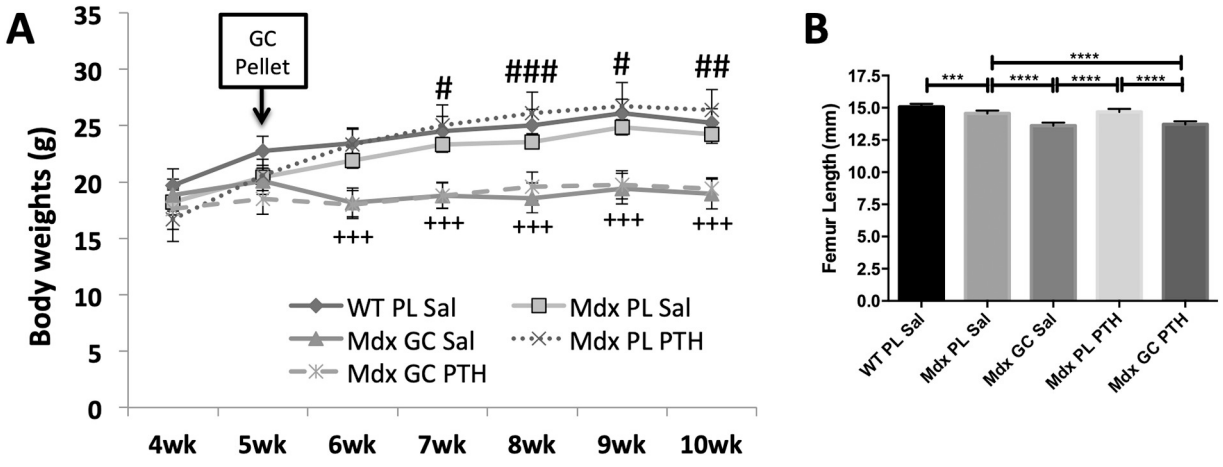

Fig. 1. Body weight and femur length. A) Weekly body weights; # Mdx PL PTH compared to Mdx PL Sal; + Mdx GC SAL and Mdx GC PTH compared to Mdx PL Sal ($^{\#}p < 0.05$; $^{\#\#}p < 0.01$; $^{\#\#\#}$, $^{+++}p < 0.001$) B) femur length at 10 weeks of age. (**p < 0.01; ***p < 0.001; ****p < 0.0001).

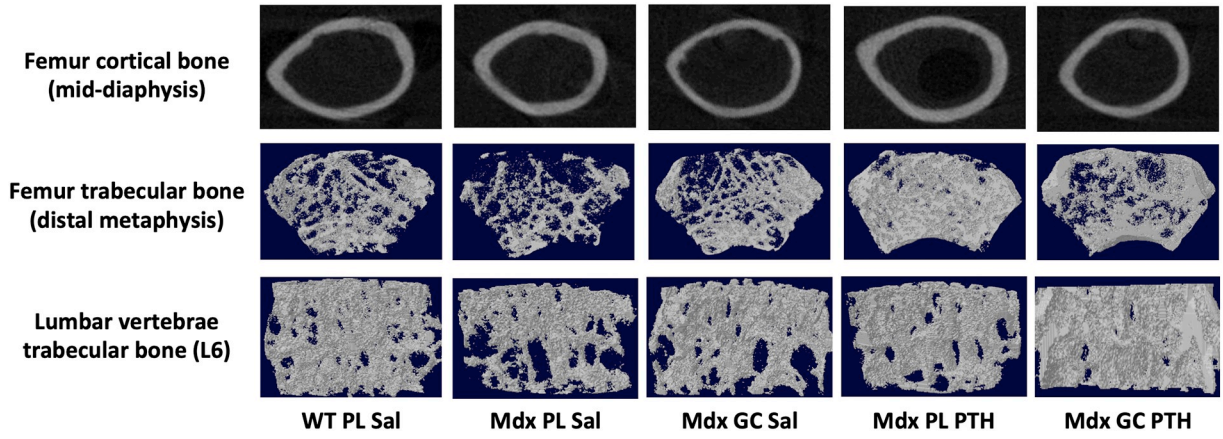

Fig. 2. Representative MicroCT images of femur cortical bone, trabecular bone in femur metaphysis, and lumbar vertebral (L6) trabecular bone. Cross-sections of femur cortical shaft at mid-diaphysis (upper panels), trabecular bone below the growth plate in distal femur (middle panels), and lumbar vertebral (L6) trabecular bone between growth plates (lower panels).

stiffness and modulus (Table 6). Again, despite the minimal effect of glucocorticoids on trabecular bone microarchitecture, lumbar vertebrae in glucocorticoid treated Mdx mice were weaker and required significantly less energy to fail, suggesting glucocorticoids negatively affecting trabecular bone mechanical properties. On the other hand, PTH positively affected mechanical properties of lumbar vertebrae by increasing strength, energy to fail, stiffness, and modulus (Table 6), again with minimal improvements on trabecular microarchitecture in L6 vertebrae (Table 4). The smaller Tb.Pf in vertebrae of PTH treated mice is indicative or more connected trabeculae that correlated with increased toughness of L6 assessed by vert compression test. Co-treatment of glucocorticoids and PTH resulted in significant improvements in all parameters except stiffness and modulus, which were still greater than control Mdx mice.

3.4. Bone turnover

TRAP-positive osteoclasts residing on endocortical bone surfaces were not significantly different for Mdx mice compared to WT (Fig. 3A, B). Five weeks of glucocorticoid treatment significantly increased endocortical osteoclast number and surface, while PTH treatment also increased the number of osteoclasts but to a lesser extent than glucocorticoids. Surprisingly, in the presence of glucocorticoids, PTH treatment significantly suppressed osteoclast number and surface, suggesting that PTH counteracted glucocorticoid-induced increases in bone resorption. This is reflected in cortical bone microarchitecture, where PTH treatment in the presence of glucocorticoids partially prevented glucocorticoid-induced cortical bone loss.

In trabecular bone of tibiae, osteoclast number and surface were significantly increased in Mdx mice, while glucocorticoids did not further increase the osteoclasts (Fig. 3A, C). PTH treatment, with and without glucocorticoids, significantly decreased osteoclast number and surface on trabecular surfaces. This phenomenon suggests that bone increases with PTH in the presence of glucocorticoids are partially the result of decreasing bone resorption.

Although the number of osteoblasts or osteocytes in trabecular bone did not significantly change, prominent decreases in osteoid volume, mineralizing surface, and bone formation rates were found with glucocorticoid treatment of Mdx mice (Fig. 3D–G). As expected, PTH treatment significantly increased osteoblast number, osteoid volume, and mineralizing surface. Even in the presence of glucocorticoids PTH significantly improved osteoid volume compared to glucocorticoid treated Mdx mice, and osteoblast number and bone formation rate compared to both glucocorticoid treated and control Mdx groups. Thus, the PTH treatment was effective in reversing deleterious effects of glucocorticoids on bone formation.

3.5. In vitro culture of bone marrow stromal cell derived osteoclasts

We next assessed if the mouse strain or treatments of mice *in vivo* altered the osteoclast potential of bone marrow cells in culture without glucocorticoids or PTH. After 4 days of bone marrow stromal cell culture in control medium, hematopoietic cells were collected and osteoclastogenesis was induced with M-CSF and RANKL cytokines. Similar to osteoclasts *in vivo*, TRAP-positive, multi-nucleated (> 3 nuclei) osteoclasts *in vitro* were also significantly increased in Mdx mice (Fig. 4). The effect of glucocorticoid treatment *in vivo* was seen in the *in vitro* cultures where osteoclasts were significantly larger (Fig. 4). PTH treatment of Mdx mice *in vivo*, had no effect on osteoclast numbers *in vitro* but PTH treatment *in vivo* did prevent glucocorticoid-induced increases in osteoclast size (Fig. 4).

3.6. Assessment of the dystrophic muscle phenotype

Grip strength was measured on a weekly basis and analysis of the collective data showed a significant effect of time on increasing grip

Table 2
Micro-CT cortical bone parameters in femur mid-diaphysis.

	WT PL Sal	Mdx PL Sal	Mdx GC Sal	Mdx PL PTH	Mdx GC PTH
Volumetric BMD (g/cm^3)	1.20 ± 0.03	1.20 ± 0.04	1.17 ± 0.02	1.18 ± 0.04	1.18 ± 0.03
Periosteal perimeter (mm)	11.46 ± 0.95	10.36 ± 0.62^{a***}	10.29 ± 0.30	10.91 ± 0.40	10.35 ± 0.25
Cortical thickness (mm)	0.113 ± 0.011	0.115 ± 0.007	0.085 ± 0.008^{b***}	0.133 ± 0.008^{b,c***}	0.097 ± 0.008 ^{b,d***,c*}
Cross-sectional bone area (mm^2)	0.649 ± 0.082	0.600 ± 0.043	0.439 ± 0.046^{b***}	0.725 ± 0.027^{b,c***}	0.507 ± 0.034^{b***,c**,d***}
Anterior-posterior diameter (mm)	1.45 ± 0.05	1.36 ± 0.03^{a***}	1.35 ± 0.04	1.44 ± 0.04^{b,c***}	1.40 ± 0.03
Medial-lateral diameter (mm)	2.04 ± 0.07	1.89 ± 0.06	1.83 ± 0.06	2.02 ± 0.05^{b,c***}	1.86 ± 0.05^{d***}

Values represent mean ± SD. (a, compared to WT PL Sal; b, compared to Mdx PL Sal; c, compared to Mdx GC Sal; d, compared to Mdx PL PTH) (*p < 0.05; **p < 0.01; ***p < 0.001).

Table 3
Micro-CT trabecular bone parameters in distal femur.

	WT PL Sal	Mdx PL Sal	Mdx GC Sal	Mdx PL PTH	Mdx GC PTH
vBMD (g/cm^3)	0.147 ± 0.018	0.107 ± 0.015^{a**}	0.150 ± 0.017^{b**}	0.191 ± 0.060^{b***}	0.142 ± 0.016^{b,d*}
BV/TV (%)	5.91 ± 1.22	3.04 ± 1.06^{a***}	6.81 ± 1.36^{b***}	14.04 ± 6.22^{b***}	10.15 ± 0.80^{b***,c,d*}
Tb.N. (mm^{-1})	2.35 ± 0.38	1.29 ± 0.36^{a***}	2.70 ± 0.54^{b***}	4.54 ± 2.09^{b***,c**}	3.02 ± 0.26^{b***,d**}
Tb.Th (μm)	0.025 ± 0.001	0.023 ± 0.002	0.025 ± 0.001	0.031 ± 0.001^{b,c***}	0.033 ± 0.001^{b,c***}
Tb.Sp (μm)	0.180 ± 0.011	0.232 ± 0.020^{a*}	0.198 ± 0.020	0.217 ± 0.065	0.264 ± 0.028^{c**,d*}
SMI	2.00 ± 0.09	2.18 ± 0.08	1.77 ± 0.09^{b***}	1.31 ± 0.33^{b***,c***}	1.50 ± 0.14^{b***,c*}
Tb.Pf	22.33 ± 6.29	37.44 ± 11.31^{a**}	11.31 ± 5.2^{b***}	15.40 ± 13.79^{b***,c***}	5.61 ± 5.58^{b***,c***,d*}

vBMD, volumetric bone mineral density; BV/TV, percent bone volume; Tb.N, trabecular number; Tb.Th, trabecular thickness; Tb.Sp, trabecular separation; SMI, structure model index; Tb. Pf, trabecular bone pattern factor. Values represent mean ± SD. (a, compared to WT PL Sal; b, compared to Mdx PL Sal; c, compared to Mdx GC Sal; d, compared to Mdx PL PTH) (*p < 0.05; **p < 0.01; ***p < 0.001).

Table 4
Micro-CT trabecular bone parameters in lumbar vertebrae (L6).

	WT PL Sal	Mdx PL Sal	Mdx GC Sal	Mdx PL PTH	Mdx GC PTH
vBMD (g/cm^3)	0.24 ± 0.02	0.21 ± 0.02^{a*}	0.21 ± 0.03	0.22 ± 0.03	0.27 ± 0.03^{b,c***,d*}
BV/TV (%)	13.99 ± 3.50	10.62 ± 3.90^{a*}	10.67 ± 2.28	13.24 ± 4.12	17.62 ± 4.97^{b,c**}
Tb.N. (mm^{-1})	4.04 ± 0.82	3.32 ± 0.98	3.32 ± 0.56	3.78 ± 0.94	4.66 ± 0.99^{b,c*}
Tb.Th (μm)	0.034 ± 0.002	0.031 ± 0.002^{a*}	0.032 ± 0.003	0.035 ± 0.002 ^{b*}	0.037 ± 0.003^{b,c***}
Tb.Sp (μm)	0.159 ± 0.010	0.179 ± 0.016^{a*}	0.171 ± 0.017	0.191 ± 0.019	0.159 ± 0.013^{d***}
SMI	1.30 ± 0.16	1.51 ± 0.15^{a*}	1.56 ± 0.10	1.17 ± 0.17^{b,c***}	0.87 ± 0.20^{b,c***,d**}
Tb.Pf	−9.82 ± 5.39	−1.16 ± 6.38^{a**}	1.11 ± 3.54	−16.04 ± 6.50^{b,c***}	−22.61 ± 5.05^{b,c***}

vBMD, volumetric bone mineral density; BV/TV, percent bone volume; Tb.N, trabecular number; Tb.Th, trabecular thickness; Tb.Sp, trabecular separation; SMI, structure model index; Tb.Pf, trabecular bone pattern factor. Values represent mean ± SD. (a, compared to WT PL Sal; b, compared to Mdx PL Sal; c, compared to Mdx GC Sal; d, compared to Mdx PL PTH) (*p < 0.05; **p < 0.01; ***p < 0.001).

Table 5
Mechanical parameters of cortical bone at femur mid-diaphysis.

	WT PL Sal	Mdx PL Sal	Mdx GC Sal	Mdx PL PTH	Mdx GC PTH
Ultimate load (N)	16.90 ± 2.33	15.85 ± 1.73	10.87 ± 1.51^{b***}	18.83 ± 1.78^{c***}	12.57 ± 1.93^{b**,d***}
Fail displacement (mm)	0.89 ± 0.15	0.46 ± 0.22^{a*}	0.47 ± 0.39	0.51 ± 0.31	0.31 ± 0.08
Energy to fail (mJ)	9.521 ± 3.84	5.128 ± 2.47^{a*}	2.656 ± 1.54^{b*}	6.812 ± 4.08^{c***}	2.747 ± 0.69^{d**}
Stiffness (N/mm)	106.4 ± 39.2	125.4 ± 27.1	74.50 ± 10.2^{b**}	164.0 ± 27.2^{b*,c***}	107.5 ± 21.5^{c*,d**}
Ultimate stress (MPa)	126.4 ± 13.9	147.3 ± 15.9	128.2 ± 18.8	138.8 ± 10.6	128.3 ± 18.9
Failure strain (%)	21.64 ± 3.68	10.48 ± 1.56^{a*}	10.74 ± 2.95	12.36 ± 2.36	7.249 ± 0.58
Toughness (MPa)	17.36 ± 7.34	9.03 ± 2.83^{a**}	5.26 ± 1.22^{b*}	15.05 ± 6.14^{b*,c***}	8.35 ± 1.64^{c*,d**}
Modulus (MPa)	4518 ± 871	5069 ± 1039	3306 ± 736^{b**}	4838 ± 1152^{c**}	4741 ± 1163^{c*}

Values represent mean ± SD. (a, compared to WT PL Sal; b, compared to Mdx PL Sal; c, compared to Mdx GC Sal; d, compared to Mdx PL PTH) (*p < 0.05; **p < 0.01; ***p < 0.001).

Table 6
Mechanical parameters lumbar vertebrae (L6).

	WT PL Sal	Mdx PL Sal	Mdx GC Sal	Mdx PL PTH	Mdx GC PTH
Ultimate load (N)	15.49 ± 2.75	11.54 ± 1.66^{a*}	8.68 ± 2.03	22.61 ± 3.11^{b,c***}	23.23 ± 4.01^{b,c***}
Fail displacement (mm)	0.481 ± 0.24	0.508 ± 0.20	0.310 ± 0.14	0.737 ± 0.39^{c***}	0.700 ± 0.31^{c***}
Energy to fail (mJ)	4.89 ± 2.22	3.61 ± 1.18	1.73 ± 1.01^{b**}	8.38 ± 4.58^{b***,c***}	11.21 ± 7.09^{b***,c***}
Stiffness (N/mm)	90.17 ± 36.81	35.81 ± 9.30^{a***}	61.68 ± 11.10	67.27 ± 25.66^{b*}	92.21 ± 42.81^{b***}
Ultimate stress (MPa)	19.41 ± 3.30	16.41 ± 2.08	13.05 ± 2.52^{b*}	26.19 ± 4.79^{b,c***}	26.56 ± 4.32^{b,c***}
Failure strain (%)	40.60 ± 22.34	46.37 ± 20.73	33.66 ± 13.38	64.12 ± 39.97	77.31 ± 27.22^{c***}
Toughness (MPa)	4.91 ± 2.44	4.72 ± 1.94	2.85 ± 1.56	9.013 ± 2.11^{c***}	13.89 ± 2.13^{b,c***}
Modulus (MPa)	102.6 ± 53.46	53.55 ± 13.50^{a*}	82.11 ± 41.83	112.8 ± 33.09^{b**}	99.80 ± 38.64^{b*}

Values represent mean ± SD. (a, compared to WT PL Sal; b, compared to Mdx PL Sal; c, compared to Mdx GC Sal; d, compared to Mdx PL PTH) (*p < 0.05; **p < 0.01; ***p < 0.001).

strength in all the mice (Fig. 5A). Grip strength of Mdx mice was significantly lower than that of WT mice. With glucocorticoids, PTH, and co-treatments, grip strength was significantly improved, although no additional effect was seen with co-treatment (Fig. 5A). Voluntary treadmill running time was drastically lower in Mdx mice compared to WT mice. This was improved significantly in glucocorticoid treated Mdx mice compared to Mdx controls and further enhanced with additional PTH treatment, despite minimal effect of PTH treatment by itself (Fig. 5B). The beneficial effect of glucocorticoids was also seen in the reduction in total serum creatine kinase activity (CK). PTH alone did not cause any notable effect on CK activity levels and it did not interfere with the effects of glucocorticoids to reduce CK levels in mice co-treated with PTH and glucocorticoids (Fig. 5C).

Evidence of muscle degeneration and regeneration was seen in the Mdx mice by increased variability in muscle fiber size and fibers with central nuclei (Fig. 5D). Glucocorticoids significantly improved muscle

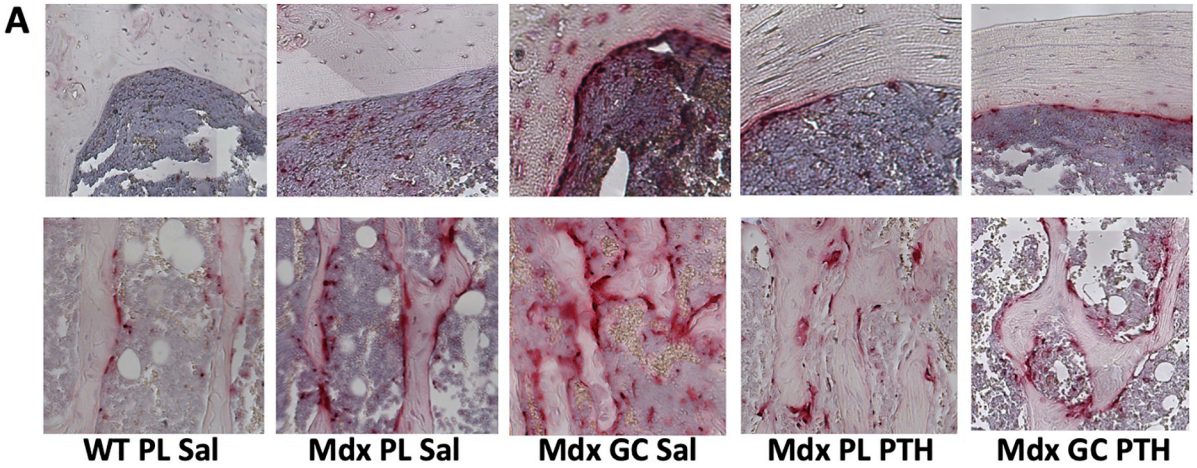

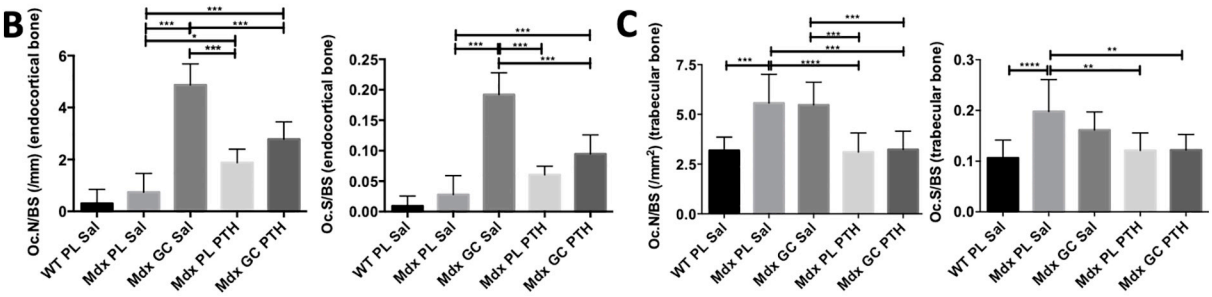

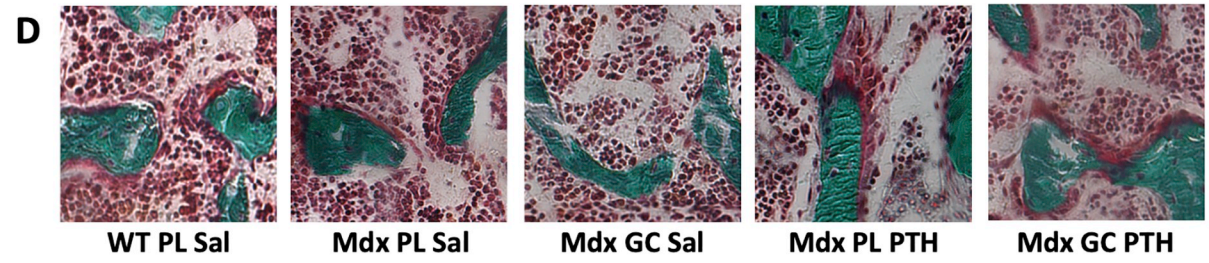

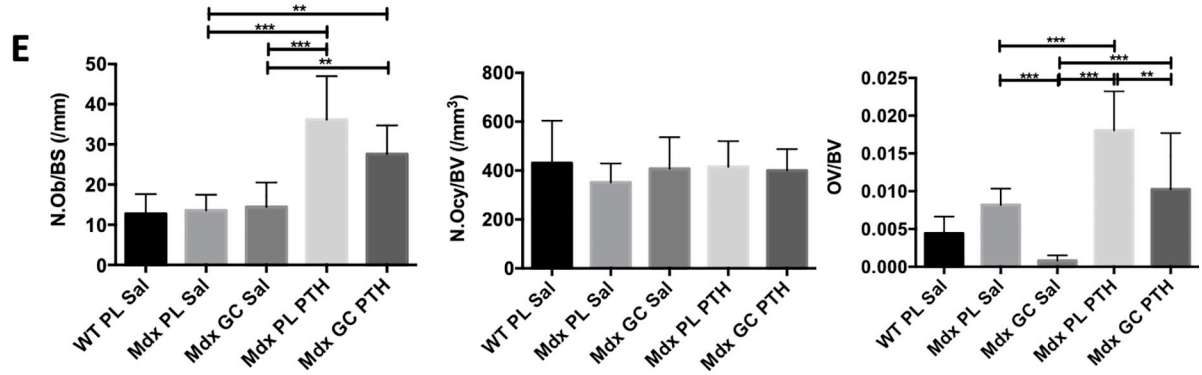

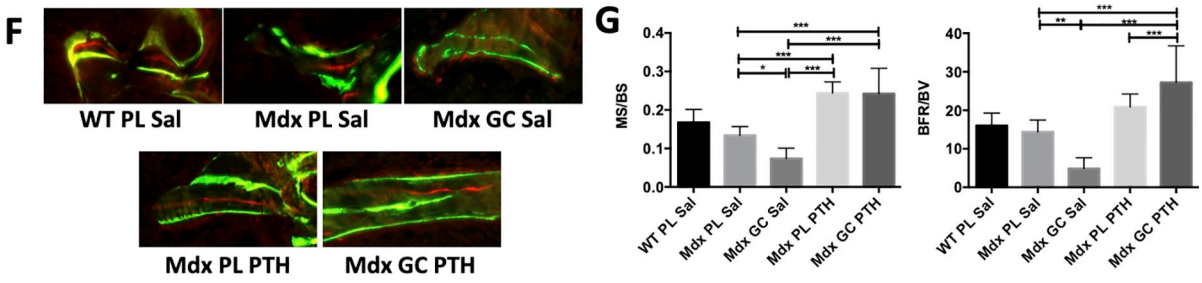

(caption on next page)

Fig. 3. Histological analyses of bone. A) Representative TRAP-stained images of decalcified endocortical bone of tibiae (top panels) and proximal tibia trabecular bone (bottom panels). B) Measurements of TRAP-stained osteoclasts on endocortical bone of tibiae; Oc.S/BS, osteoclast surface per bone surface; N.Oc/BS, osteoclast number per bone surface. C) Measurements of TRAP-stained osteoclasts on trabecular bone of tibia proximal metaphysis. D) Representative Goldner's Trichrome stained distal femur trabecular bone. E) Measurements of static histology analyses; N.Ob/BS, osteoblast number per bone surface; N.Ocy/BV, osteocyte number per bone volume; OV/BV, osteoid volume per bone volume. F) Representative calcein-labeled sections of distal femur. G) Measurements of dynamic histology analyses; MS/BS, mineralizing surface per bone surface; BFR/BV, bone formation rate per bone volume. Values represent mean ± SD (*p < 0.05; **p < 0.01; ***p < 0.001; ****p < 0.001).

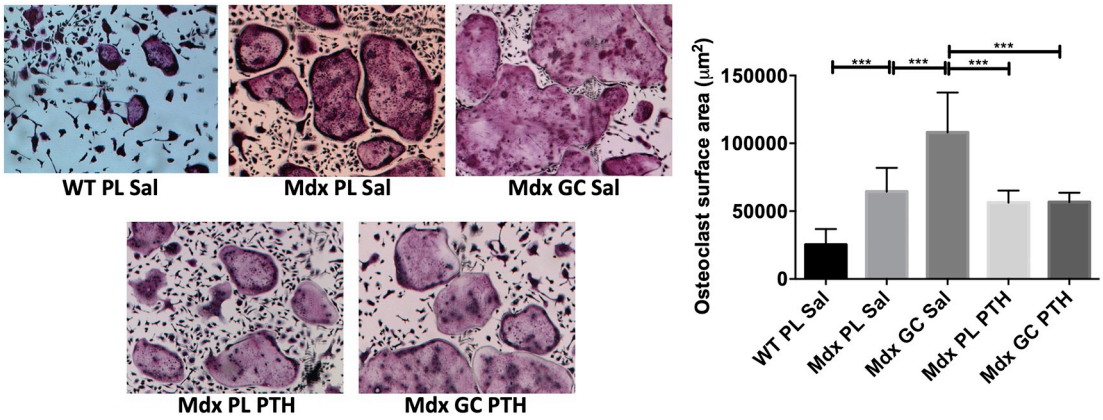

Fig. 4. *In vitro* osteoclastogenesis from bone marrow hematopoietic osteoclast precursor cells. Representative TRAP stained osteoclasts *in vitro* (10× magnification) with a histogram of average surface area of all osteoclasts that were TRAP positive and had at least 3 nuclei. (*p < 0.05; ***p < 0.001).

fiber turnover as seen in both of these parameters, while PTH treatment significantly decrease only the central nuclei containing fiber percentage (Fig. 5E). In the presence of glucocorticoids, PTH further enhanced the percentage of fibers with central nuclei.

Muscle fibers are divided into several types that can be distinguished histologically with staining for ATPase. Type 1 (slow twitch fibers) are dark stained under these acidic conditions as shown in Fig. 5F, slow twitch type 2a appear as very light fibers while type 2b are gray and intermediate type 2c are dark gray. When we examined the fiber types in tibialis anterior muscle, we saw a decrease in type 1 and type 2a fibers and an increase in type 2b and 2c fibers in Mdx mice (Fig. 5G). With glucocorticoid treatment, type 1 fibers were significantly increased, in agreement with the longer running time in Mdx mice on glucocorticoids. Type 2c intermediate fibers were significantly reduced by all treatments, and to a greatest extent in the co-treated group. However, some grouping of similar fiber types was still observed in all treatment groups of Mdx muscle, which is a typical feature of dystrophic muscle [25]. Groupings of muscle fibers occur as a result of muscle damage, where the remaining healthy fibers sprout out in the place of degenerated fibers. The same types of fibers, then, are found adjacent to each other in a group ("muscle fiber grouping"), instead of being scattered throughout the muscle. Nonetheless, intermittent PTH treatment in the presence of glucocorticoids maintained or further improved the positive effects of glucocorticoids on dystrophic muscle phenotype.

In the quadriceps muscle the mRNA expressions of a number of genes known to be upregulated in Mdx muscle were examined. The regeneration marker insulin-like growth factor-2 (*Igf2*) as well as markers of fibrosis collagen 1 (*Col1a*) and periostin (*Postn*) were down-regulated with glucocorticoids as well as in co-treatment without additive effects (Fig. 6A–C). Inflammatory markers, lectin galactose binding soluble 3 (*Lgals3*) and osteopontin (*Spp1*), were both highly up-regulated in Mdx muscle and significantly decreased with glucocorticoid treatment, and for *SPP1* this was enhanced with co-treatment with PTH (Fig. 6D, E). Fibroblast growth factor-21 (*Fgf21*) is a regulator of lipid and glucose metabolism and has been shown to be up-regulated in muscular dystrophy [6], here it was also shown to be up-regulated bin Mdx muscle and this was significantly decreased by both prednisone and PTH treatments (Fig. 6F). We also examined the expression of several cytokines from muscle that could potentially regulate bone. These included interlukin-6 (*IL-6*) that was not increased in Mdx muscle but was significantly suppressed by both prednisone and PTH treatments (Fig. 6G) and interlukin-1β (*IL-1β*) that was increased in Mdx muscle and suppressed only by prednisone (Fig. 6H). Three other gene expression levels were examined and not found to be up-regulated in Mdx muscle and not regulated by any of the treatments of the mice; these were the cytokine transforming growth factor α (*TNFα*), the regulator of osteoclasts receptor activator of nuclear factor kappa B ligand (*Tnfsf11*) and the extracellular matrix protein osteonectin (*Sparc*) (Fig. 6I–K).

4. Discussion

Duchenne Muscular Dystrophy (DMD) patients are consistently reported to have compromised bone health with lower BMD and high fracture incidence. With glucocorticoid treatment, BMD is further reduced, especially in vertebrae, resulting in significantly higher vertebral fracture rates. Thus far, calcium and vitamin D supplementation, the suggested treatments, have limited effect as even high dose vitamin D supplementation still leaves 38% of DMD patients with insufficient levels of vitamin D [26] and higher fracture incidence persists [27]. Intervention to improve bone health, preferably before the development of glucocorticoid-induced osteoporosis has been limited. One study on prophylactic use (during glucocorticoid treatment but before fracture) of oral risedronate in glucocorticoid treated DMD boys showed that BMD was maintained but the fracture incidence was not improved [28]. Similarly, in our previous study using Mdx mice, co-treatment with pamidronate at the initiation of glucocorticoid treatment significantly improved bone mineral density and micro-architecture, but not biomechanical properties of bone [13]. Our more recent study showed that administering bisphosphonates before exposure to glucocorticoids could improve bone strength, although not to the level seen without glucocorticoid treatment [14]. In our previous study [13] in 13 week old Mdx mice we saw no significant effect of mouse phenotype or glucocorticoids on trabecular bone mass (bone volumetric density or bone volume percent) in either the distal femur or lumbar vertebrae. In the current study Mdx mice were examined earlier at 10 weeks of age where the Mdx mice had significantly lower

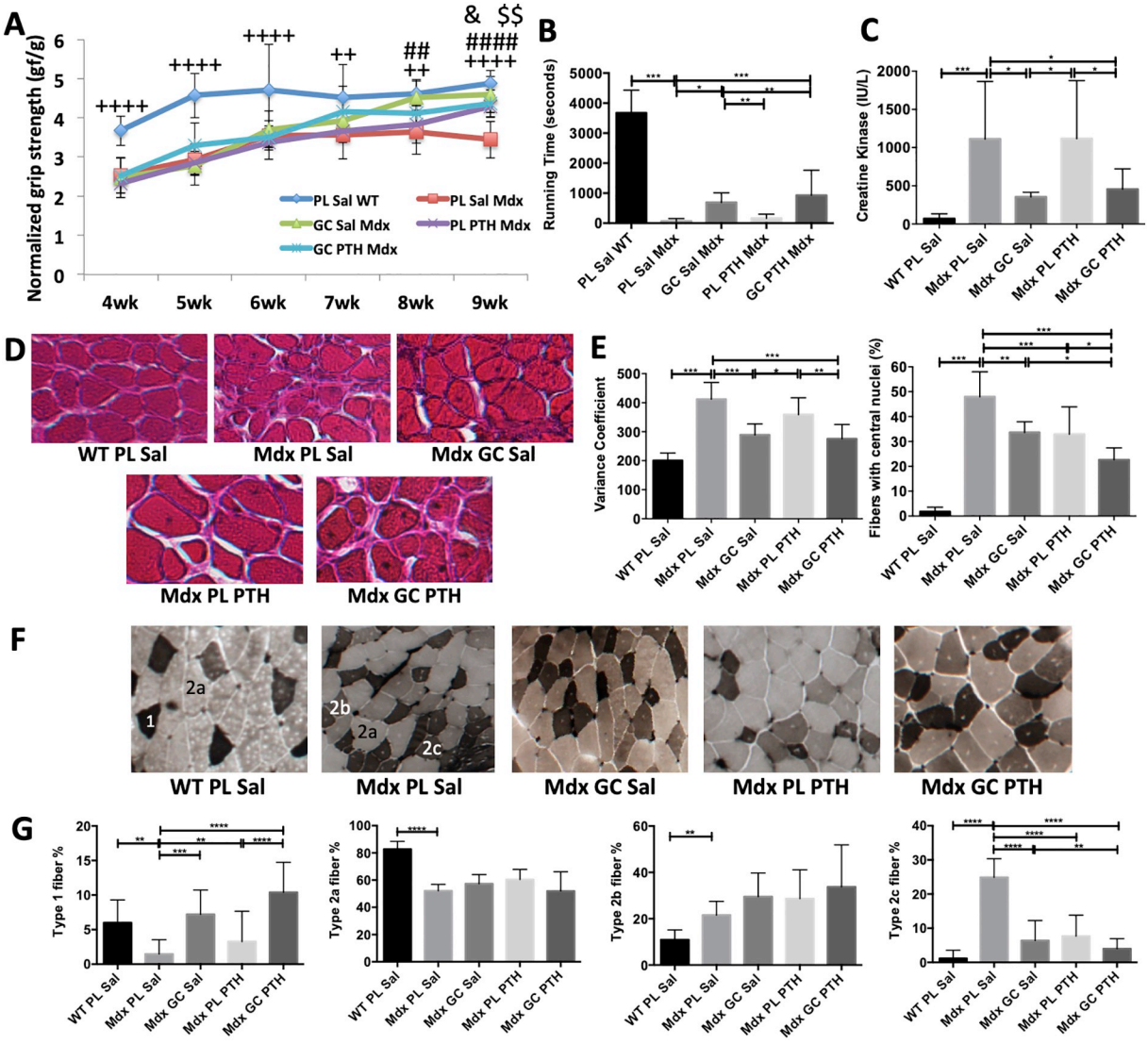

Fig. 5. Treatment effects on muscles. A) Weekly grip strength normalized to body weight. + Mdx PL Sal compared to WT PL Sal ($^{++}p < 0.01$; $^{++++}p < 0.001$); # Mdx GC Sal compared to Mdx PL Sal ($^{\#\#}p < 0.01$; $^{\#\#\#\#}p < 0.001$); & Mdx PL PTH compared to Mdx PL Sal); $Mdx GC PTH compared to Mdx PL Sal). B) Treadmill running time. C) Serum creatine kinase activity level. D) Representative images of H&E stained diaphragm sections. E) Variance coefficient of muscle diameters and percentage of fibers with central nuclei. F) Representative images of ATPase (pre-incubation at pH 4.6) stained cryo-sections of tibialis anterior, with examples of the various fiber types identified in the first two panels. G) The percentages of each muscle fiber type. Values represent mean ± SD (*$p < 0.05$; **$p < 0.01$; ***$p < 0.001$; ****$p < 0.001$).

trabecular bone mass compared to WT mice and here glucocorticoids significantly increased trabecular vBMD and BV/TV. While we do not have any evidence to determine how glucocorticoids had this positive effect in these younger Mdx mice it is possible that at 10 weeks of age there is more inflammation in Mdx mice and that glucocorticoids decreased this inflammation and therefore had indirect positive effects on trabecular bone mass. There were also site-specific effects of the Mdx stain on bone in our study where trabecular bone in the distal femur was more profoundly affected than in lumbar vertebrae. Similarly glucocorticoids affected these two sites differently. In the distal femur prednisone normalized trabecular bone to the level seen in WT mice while in lumbar vertebrae there was no effect. We have no explanation for this difference. However, there are several other examples of site-specific effects of glucocorticoids and PTH on trabecular bone in the literature [29,30], however there is currently no understanding of mechanisms that account for these differences.

The decrease in bone early in muscular dystrophy suggests that anabolic therapy to improve bone mass and strength in DMD may be a useful approach to inhibit the negative effects of dystrophic muscle and glucocorticoid therapy early in the disease. Here we have assessed the effects of iPTH treatment early in bone growth in Mdx mice, something that has not been assessed in DMD patients. Our study showed positive effects of iPTH on BMD and microarchitectures of trabecular and cortical bone, as well as bone biomechanical properties, even in the presence of glucocorticoids. In these rapidly growing mice, iPTH exerted positive effects on bone by increasing the number of osteoblasts, which in turn increased bone formation rate, but we also saw suppression of osteoclast number and surface. It has previously been shown in many studies using adult mice that iPTH stimulates both bone formation and resorption, although the net effect favors bone formation, at least within the anabolic time window [31,32]. Growing bone undergoing modeling on the other hand does not couple bone formation and resorption as seen in adult bone. In growing Mdx mice there were elevated osteoclast numbers and surfaces on trabecular bone compared to WT mice, suggesting increased stimulation of osteoclasts by dystrophic muscle or factors released by muscle such as *IL-6* family cytokines or *FGF-21* as shown here and previously reported by others to be increased in Mdx mice [5,6]. This increase in osteoclasts likely accounted for the

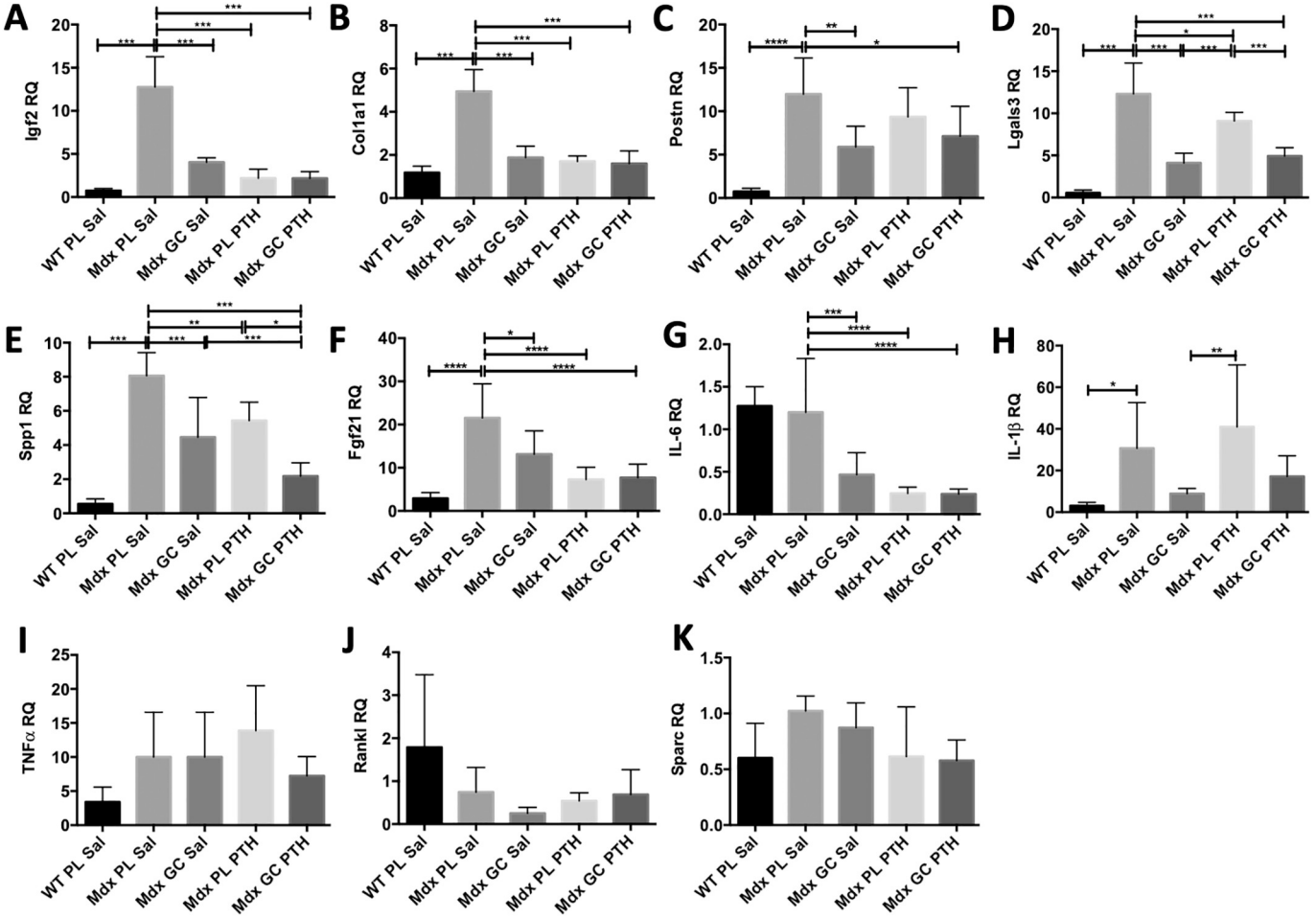

Fig. 6. Treatment effects on gene expression in skeletal muscle. Relative quantification (RQ) levels of mRNAs extracted from quadriceps muscle were assessed by qPCR. A) Insulin-like growth factor-2 (*Igf-2*). B) Collagen 1al (*Col1a1*). C) periostin (*Postn*). D) Lectin galactose binding soluble 3 (*Lgals3*). E) Osteopontin (*Spp1*). F) Fibroblast growth factor-21 (*Fgf-21*). G) Interleukin-6 (*IL-6*). H) Interleukin-1 beta (*IL-1β*). I) Tumor necrosis factor alpha (*TNFα*). J) Receptor activator of nuclear factor kappa-B ligand (*RANKL*). K) Osteonectin (*Sparc*).

decreased trabecular bone volume seen in the Mdx mice since osteoblast numbers and bone formation rates were not altered in these mice. Increased inflammation in Mdx mice and DMD patients has been suggested to play a role in bone loss by stimulating osteoclast activity [5]. While PTH can stimulate osteoclasts through its ability to increase RANKL expression from osteoblasts, in the Mdx mice iPTH treatment decreased osteoclasts. This effect may have been the result of PTH inhibition of inflammation as *Spp1*, *IL-6*, *FGF-21* and *Lgals3*, all pro-inflammatory markers were all upregulated in dystrophic Mdx muscle and significantly decreased in mice treated with iPTH. Along with a robust increase in osteoblast numbers and activity iPTH treatment resulted in more than double the amount of trabecular bone. Importantly, the increase in osteoblasts and decrease in osteoclasts with iPTH treatment was still seen in glucocorticoid treated Mdx mice. This resulted in robust increases in trabecular bone with tougher, stronger trabeculae counteracting the effects of glucocorticoids.

Cortical bone size and mineral density were only mildly affected in the Mdx mice in comparison to WT mice, however, the quality of the bone was significantly decreased with lower energy to fail and toughness and this was further exacerbated by glucocorticoid treatment. Glucocorticoids also decrease cortical thickness and cross-sectional area and all of these were improved by iPTH treatment. Endocortical surfaces in Mdx mice treated with glucocorticoids showed large increases in osteoclasts and these were again decreased by iPTH treatment. This inhibitory effect of PTH on osteoclasts has not been reported previously and here we show that it can also be seen when osteoclasts were differentiated from bone marrow precursors *in vitro*. We have previously reported the effect of *in vivo* glucocorticoid treatment on osteoclast size when differentiated *in vitro* [13], the mechanism of this effect as well as the ability of iPTH to inhibit it is unknown and is currently under investigation.

Our results are consistent with the positive effects of iPTH treatment in glucocorticoid-induced osteoporosis in adult rodent bone with significant increases in bone formation rate, bone strength, and cortical and trabecular bone microarchitectures [33]. Similarly, in glucocorticoid-induced osteoporotic patients who did not respond to bisphosphonates, iPTH decreased fractures and increased bone density [34]. Potential benefits of PTH on growing bone have also been shown in Mdx mice using black bear PTH, with significantly increased trabecular bone mass in long bones [35]. Although, in growing FVB mice, minimal effects of iPTH in the presence of glucocorticoids has been reported [36], the lack of improvements with PTH in that study compared to ours and others in Mdx mice could be the result of the differences in mouse strain or dosing regimen.

In addition to bone, we show here that iPTH treatment can improve dystrophic muscle in Mdx mice. A study by Kimura and Yoshioba suggested that the PTH type 1 receptor is required for myocyte differentiation [37] and here we showed that PTH treatment improved muscle regeneration and improved muscle strength and decreased inflammation. Dystrophin deficiency is known to affect type 2 fibers [38], which was confirmed here in our study. But we also found a significant decrease in type 1 fibers, with a significant increase of type 2c

intermediate fibers and groupings of the same muscle fiber types, which are the typical characteristics of dystrophic muscle. In this study, we showed the effects of glucocorticoids on distribution of muscle fiber types in Mdx mice for the first time. The increase in type 1 fibers with glucocorticoids is consistent with the significantly longer running times in glucocorticoid-treated Mdx mice in our study. In addition, the significant reduction in type 2c fibers suggests that Mdx muscle has a limited capacity to differentiate muscle properly, and that glucocorticoids, PTH, and co-treatments aid in myocyte differentiation. It has been suggested that glucocorticoids may improve myogenic precursor cells or myoblast proliferation, as well as myotube formation in Mdx mice, helping to offset the typical effect of glucocorticoids to increase muscle atrophy, resulting in a net increase in muscle regeneration and growth in mdx mice [38–41]. The important role of PTH in myocyte differentiation has been suggested [37], but the interaction between glucocorticoids and PTH as seen here in decreased expression of *Spp1* (osteopontin) and decreased fibers with central nuclei in Mdx muscle needs further investigation.

Despite the positive effects of iPTH treatment in bone, its use in children with osteoporosis raises concerns of osteosarcoma development. There has been one case study report of teriparatide use in a 20 year-old DMD patient with multiple vertebral fractures [42]. Once daily use of teriparatide showed positive effects not only on bone health and managing bone pain, but also on the general health and physical function in this patient, suggesting teriparatide as a potential alternative for DMD patients with compromised bone.

In summary, this study shows, for the first time, the therapeutic potential of intermittent PTH treatment of glucocorticoid-induced osteoporosis in a mouse model of DMD during rapid growth. With glucocorticoids, cortical bone thickness and mechanical properties were undermined and the additional intervention with PTH counteracted glucocorticoid-induced suppression of osteoblast activity and significantly improved cortical thickness and toughness. Trabecular bone that was significantly decreased in Mdx mice was greatly increased by PTH treatment and all biomechanical parameters, except for stiffness, were significantly improved in vertebrae. Furthermore, the addition of PTH treatment either maintained or had further positive effects on dystrophic muscle, especially muscle endurance.

As PTH treatment had profound effects on bone and also maintained or further improved dystrophic muscle, the use of intermittent PTH should be considered in glucocorticoid-treated boys with DMD.

Acknowledgments

This work was supported by a grant to MDG and JM from the Canadian Institutes of Health Research (CIHR MOP-123265), S-HY received support from the Ontario Graduate Studies Award.

References

[1] M. Koenig, et al., The molecular basis for Duchenne versus Becker muscular dystrophy: correlation of severity with type of deletion, Am. J. Hum. Genet. 45 (1989) 498–506.
[2] H.J.A. Van Ruiten, et al., Why are some patients with Duchenne muscular dystrophy dying young: an analysis of causes of death in North East England, Eur. J. Paediatr. Neurol. 20 (2016) 904–909.
[3] C.M. Larson, R.C. Henderson, Bone mineral density and fractures in boys with Duchenne muscular dystrophy, J. Pediatr. Orthop. 20 (2000) 71–74.
[4] M.L. Bianchi, et al., Bone mineral density and bone metabolism in Duchenne muscular dystrophy, Osteoporos. Int. 14 (2003) 761–767.
[5] A. Rufo, et al., Mechanisms inducing low bone density in Duchenne muscular dystrophy in mice and humans, J. Bone Miner. Res. 26 (2011) 1891–1903.
[6] S. Zhou, et al., Altered bone-regulating myokine expression in skeletal muscle of Duchenne muscular dystrophy mouse models, Muscle Nerve 58 (2018) 573–582.
[7] D. Heymann, A.V. Rousselle, gp130 cytokine family and bone cells, Cytokine 12 (2000) 1455–1468.
[8] H. Yasuda, et al., Osteoclast differentiation factor is a ligand for osteoprogerin/osteogenesis-inhibitory factor and is identical to TRANCE/RANKL, Proc. Natl. Acad. Sci. U. S. A. 95 (1998) 3597–3602.
[9] E. Matthews, et al., Corticosteroids for the treatment of Duchenne muscular dystrophy, Cochrane Database Syst. Rev. 5 (2016) CD003725.
[10] J.E. Bothwell, et al., Vertebral fractures in boys with Duchenne muscular dystrophy, Clin. Pediatr. 42 (2003) 353–356.
[11] W.M. King, et al., Orthopedic outcomes of long-term daily corticosteroid treatment in Duchenne muscular dystrophy, Neurology 68 (2007) 1607–1613.
[12] S. Houde, et al., Deflazacort use in Duchenne muscular dystrophy: an 8-year follow-up, Pediatr. Neurol. 38 (2008) 200–206.
[13] S.H. Yoon, J. Chen, M.D. Grynpas, J. Mitchell, Prophylactic pamidronate partially protects from glucocorticoid-induced bone loss in the mdx mouse model of Duchenne muscular dystrophy, Bone 90 (2016) 168–180.
[14] J. Chen, S.H. Yoon, M.D. Grynpas, J. Mitchell, Pre-treatment with pamidronate improves bone mechanical properties in Mdx mice treated with glucocorticoids, Calcif. Tissue Int. (2018) Oct 9. (Epub ahead of print).
[15] M. Pazianas, Anabolic effects of PTH and the 'anabolic window', Trends Endocrinol. Metab. 26 (2015) 111–113.
[16] K.G. Saag, et al., Effects of teriparatide versus alendronate for treating glucocorticoid-induced osteoporosis: thirty-six-month results of a randomized, double-blind, controlled trial, Arthritis Rheum. 60 (2009) 3346–3355.
[17] E. Canalis, G. Mazziotti, A. Giustina, J.P. Bilezikian, Glucocorticoid-induced osteoporosis: pathophysiology and therapy, Osteoporos. Int. 18 (2007) 1319–1328.
[18] J. Manning, D. O'Malley, What has the mdx mouse model of Duchenne muscular dystrophy contributed to our understanding of the disease? J. Muscle Res. Cell Motil. 36 (2015) 155–167.
[19] S.A. Novotny, et al., Bone is functionally impaired in dystrophic mice but less so that skeletal muscle, Neuromuscul. Disord. 21 (2011) 183–193.
[20] M.L. Bouxsein, et al., Guidelines for assessment of bone microstructure in rodents using micro-computed tomography, J. Bone Miner. Res. 25 (2010) 1468–1486.
[21] C. Pautke, et al., Polychrome labeling of bone with seven different fluorochromes: enhancing discrimination by spectral image analysis, Bone 37 (2005) 441–445.
[22] D.W. Dempster, et al., Standardized nomenclature, symbols, and units for bone histomorphometry: a 2012 update of the report of the ASBMR Histochemistry Nomenclature Committee, J. Bone Miner. Res. 28 (2013) 2–17.
[23] J. Dubach-Powell, Quantitative Determination of Muscle Fiber Diameter (Minimal Feret's Diameter) and Percentage of Centralized Nuclei, Treat-NMD, 2014, pp. 1–16 http://www.treat-nmd.eu/research/preclinical/cmd-sops/.
[24] W.M.H. Behan, D.W. Cossar, H.A. Madden, I.C. McKay, Validation of a simple, rapid, and economical technique for distinguishing type 1 and 2 fibres in fixed and frozen skeletal muscle, J. Clin. Pathol. 55 (2002) 375–380.
[25] C. Pastoret, A. Sebille, Fibres of intermediate type 1C and 2C are found continuously in mdx soleus muscle up to 52 weeks, Histochemistry 100 (1993) 271–276.
[26] N. Perera, H. Sampaio, H. Woodhead, M. Farrar, Fracture in Duchenne muscular dystrophy: natural history and vitamin D deficiency, J. Child Neurol. 31 (2016) 1181–1187.
[27] M.L. Bianchi, et al., Low bone density and bone metabolism alterations in Duchenne muscular dystrophy: response to calcium and vitamin D treatment, Osteoporos. Int. 22 (2011) 529–539.
[28] R. Srinivasan, et al., Prophylactic oral bisphosphonate therapy in duchenne muscular dystrophy, Muscle Nerve 54 (2016) 79–85.
[29] M.C. Schulz, et al., Site-specific variations in bone mineral density under systemic conditions inducing osteoporosis in minipigs, Front. Physiol. 8 (2017) 426.
[30] R.I. Gafni, et al., Daily parathyroid hormone 1-34 replacement therapy for hypoparathyroidism induces marked changes in bone turnover and structure, J. Bone Miner. Res. 27 (2012) 1811–1820.
[31] W. Yao, et al., Glucocorticoid-induced bone loss in mice can be reversed by the actions of parathyroid hormone and risedronate on different pathways for bone formation and mineralization, Arthritis Rheum. 58 (2008) 3485–3497.
[32] R.S. Weinstein, et al., Intermittent parathyroid hormone administration counteracts the adverse effects of glucocorticoids on osteoblast and osteocyte viability, bone formation, and strength in mice, Endocrinology 151 (2010) 2641–2648.
[33] J. Iwamoto, A. Seki, Y. Sato, Effect of intermittent administration of hPTH(1-34) on cortical bone geometry in rats treated with high-dose glucocorticoids, Chin. J. Phys. 57 (2014) 231–237.
[34] N.E. Lane, et al., Bone mass continues to increase at the hip after parathyroid hormone treatment is discontinued in glucocorticoid-induced osteoporosis: results of a randomized controlled clinical trial, J. Bone Miner. Res. 15 (2000) 944–951.
[35] S.K. Gray, et al., Black bear parathyroid hormone has greater anabolic effects on trabecular bone in dystrophin-deficient mice than in wild type mice, Bone 51 (2012) 578–585.
[36] A. Postnov, et al., Glucocorticoid-induced osteoporosis in growing mice is not prevented by simultaneous intermittent PTH treatment, Calcif. Tissue Int. 85 (2009) 530–537.
[37] S. Kimura, K. Yoshioka, Parathyroid hormone and parathyroid hormone type-1 receptor accelerate myocyte differentiation, Sci. Rep. 4 (5066) (2014).
[38] C. Webster, L. Silberstein, A.P. Hays, H.M. Blau, Fast muscle fibers are preferentially affected in Duchenne muscular dystrophy, Cell 52 (1988) 503–513.
[39] A.C. Passaquin, L. Metzinger, J.J. Léger, J.M. Warter, P. Poindron, Prednisolone enhances myogenesis and dystrophin-related protein in skeletal muscle cell cultures from mdx mouse, J. Neurosci. Res. 35 (1993) 363–372.
[40] C. Angelini, E. Peterle, Old and new therapeutic developments in steroid treatment in Duchenne muscular dystrophy, Acta Myologica 31 (2012) 9–15.
[41] F. Muntoni, I. Fisher, J.E. Morgan, D. Abraham, Steroids in Duchenne muscular dystrophy: from clinical trials to genomic research, Neuromuscul. Disord. 12 (2002) 162–165.
[42] A. Catalano, et al., Effects of teriparatide on bone mineral density and quality of life in Duchenne muscular dystrophy related osteoporosis: a case report, Osteoporos. Int. 27 (2016) 3655–3659.